Journal of Power Sources 239 (2013) 443–448

Contents lists available at SciVerse ScienceDirect

Journal of Power Sources

journal homepage: www.elsevier.com/locate/jpowsour

Short communication

Electrochemical investigation of $Y_{0.5}Ca_{0.5}BaCo_{4-x}Zn_xO_7$-$Ce_{0.8}Sm_{0.2}O_2$ composite cathode materials for solid oxide fuel cells

Rui Wang, Jigui Cheng*, Qiumei Jiang, Junfang Yang, Yifang Wang, Kui Xie

School of Materials Science and Engineering, Hefei University of Technology, Hefei 230009, China

HIGHLIGHTS

- EDTA–citric (EC) method was first exploited to synthesis nanosized $Y_{0.5}Ca_{0.5}BaCo_{4-x}Zn_xO_7$ ($x = 0.3, 1.0, 1.5$) powders.
- The $Y_{0.5}Ca_{0.5}BaCo_{4-x}Zn_xO_7$ materials have relatively low TECs and are chemical stable with SDC electrolytes.
- $Y_{0.5}Ca_{0.5}BaCo_{4-x}Zn_xO_7$-SDC composites were first evaluated as cathode materials for IT-SOFC.
- Single cell with the composite cathode and SDC electrolyte has a power density of about 320 mW cm^{-2} at 700 °C.

ARTICLE INFO

Article history:
Received 1 December 2012
Received in revised form
25 March 2013
Accepted 26 March 2013
Available online 6 April 2013

Keywords:
Solid oxide fuel cell
Cathode materials
Impedance
Polarization

ABSTRACT

This paper investigates $Y_{0.5}Ca_{0.5}BaCo_{4-x}Zn_xO_7$-$Ce_{0.8}Sm_{0.2}O_2$ (SDC) composite cathode materials for intermediate temperature solid oxide fuel cells (SOFCs). The effects of Zn contents in $Y_{0.5}Ca_{0.5}BaCo_{4-x}Zn_xO_7$ materials on the electrical conductivity, electrochemical performances and thermal expansion have been systemically studied. It is found that the $Y_{0.5}Ca_{0.5}BaCo_{4-x}Zn_xO_7$ materials have good electrical conductivity. Sintered $Y_{0.5}Ca_{0.5}BaCo_3ZnO_7$ samples show a lowest thermal expansion coefficient (TEC) of about 9.3×10^{-6} K^{-1}. This makes the cathode materials well thermally compatible with SDC electrolytes. XRD results show that the $Y_{0.5}Ca_{0.5}BaCo_{4-x}Zn_xO_7$ materials are chemically stable to SDC electrolyte. Furthermore, $Y_{0.5}Ca_{0.5}BaCo_{4-x}Zn_xO_7$-SDC composite cathodes have small area specific resistance (ASR) with SDC electrolyte. The ASR value is 0.05 Ω cm^2 at 800 °C and 0.11 Ω cm^2 at 750 °C, respectively. Single solid oxide fuel cells based on the $Y_{0.5}Ca_{0.5}BaCo_3ZnO_7$-SDC (50:50) composite cathode with SDC as electrolyte and Ni/SDC as anode show maximum power density of 320 mW cm^{-2}, 260 mW cm^{-2} and 200 mW cm^{-2} at 700 °C, 650 °C and 600 °C, respectively.

1. Introduction

Over the past decades, solid oxide fuel cells (SOFCs) have become one of the promising candidates in distributed stationary power generation, auxiliary power supply in vehicles and other energy supply devices. However, there still exist some technical and economical obstacles that limit the practical use of SOFCs. In recent years, significant efforts have been devoted to decrease the operation temperature of solid oxide fuel cells (SOFCs) to reduce the manufacturing costs and to prolong the lifetime of SOFCs. One of the important ways is to develop new cathode materials, because the high electrode polarization resistance (especially cathodic polarization resistance) at reduced temperature greatly decreases cell performance. It has been shown that some perovskite-like cobaltites possess superior electrochemical activity due to their high mixed ionic-electronic conductivity and fast oxygen exchange kinetics. These perovskite materials therefore have attracted much attention for use as cathodes of SOFCs, especially at operation temperature below 800 °C [1,2]. Nevertheless, the cobalt containing oxides have a relatively high thermal expansion coefficient (TEC), which may result in the thermal dismatch between the electrode and the electrolyte [3].

Recently, a new class of cobalt oxides with formula $RBaCo_4O_7$ (R = Y, Dy-Lu), the so-called R114 phase, has been reported by several groups [4,5]. The $RBaCo_4O_7$ oxides demonstrate interesting oxygen mobility, storage capacity and electrical property, as well as relatively low thermal expansion coefficient (TEC) [6–8]. These characteristics make $RBaCo_4O_7$ attractive as cathode materials for SOFCs [9,10]. However, the reducibility of Co^{3+} at high temperature may decrease the stability of these materials above 800 °C, which may also limit their use [5,11]. Some researches have shown that substituting Y by Ca in the $YBaCo_4O_7$ materials is beneficial to the

* Corresponding author. Fax: +86 551 62901793.
E-mail addresses: jgcheng@hfut.edu.cn, jgcheng63@sina.com (J. Cheng).

0378-7753/$ – see front matter © 2013 Elsevier B.V. All rights reserved.
http://dx.doi.org/10.1016/j.jpowsour.2013.03.148

diffusion of oxygen ion in lattice and to the improvement of the electrochemical performance, but at the cost of structural stability [12]. It has been confirmed that the phase stability of $RBaCo_4O_7$ materials can be significantly enhanced by substituting Co by Zn, as reported by Hao et al. [9,13]. Therefore, it is necessary to do further researches on the $RBaCo_4O_7$ materials to optimize their structure and property. In this work, Zn is doped with various concentrations to substitute Co in $Y_{0.5}Ca_{0.5}BaCo_{4-x}Zn_xO_7$ materials to enhance the structural stability, and the effects of Zn contents on the electrochemical properties of $Y_{0.5}Ca_{0.5}BaCo_{4-x}Zn_xO_7$ materials have been studied. Composite cathode materials based on $Y_{0.5}Ca_{0.5}BaCo_{4-x}Zn_xO_7$ material were also designed and characterized, which not only demonstrates excellent structural stability but also shows reasonable electrochemical performances in solid oxide fuel cells.

2. Experimentals

2.1. Sample preparation

$Y_{0.5}Ca_{0.5}BaCo_{4-x}Zn_xO_7$ ($x = 0$, 0.3, 1.0, 1.5) powders were synthesized by a combined ethylene diamine tetraacetic acid (EDTA)-citrate complexing method. Stoichiometric chemicals were firstly mixed in a citric acid solution to form a homogeneous mixture. EDTA-ammonia solution was then added into the mixture to yield a transparent solution. The Mole ratio of critic acid:EDTA acid:-metalic ion is 1:1:1. The solution was then heated and a combustion eventually occurred. The resultant grown powders were further fired to obtain $Y_{0.5}Ca_{0.5}BaCo_{4-x}Zn_xO_7$ powders. Samaria doped ceria ($Sm_{0.2}Ce_{0.8}O_{2-\delta}$ (SDC)) powders were prepared by a co-precipitation method using cerium and samarium nitrates ($Ce(NO_3)_3$, $Sm(NO_3)_3$) as cation source and ammonia carbonate ($(NH_4)_2CO_3$) as precipitant. Cerium and samarium nitrate solution with a cation concentration of (0.1 mol L^{-1}) was first prepared. The nitrate solution was then dropped into an ammonium carbonate solution (0.1 mol L^{-1}) under mild stirring to form carbonate precipitants. After washing, the precipitates were dried at 70 °C, and calcined at 800 °C for 2 h to obtain SDC powders with fluorite structure.

Sintered $Y_{0.5}Ca_{0.5}BaCo_{4-x}Zn_xO_7$ samples with different Zn doping amount ($x = 0$, 0.3, 1.0, 1.5) were prepared by pressing the $Y_{0.5}Ca_{0.5}BaCo_{4-x}Zn_xO_7$ at a pressure of 300 MPa and fired the green compacts at 1200 °C for 5 h. Symmetrical cells with SDC as electrolytes and $Y_{0.5}Ca_{0.5}BaCo_{4-x}Zn_xO_7$ ($x = 0.3$, 1.0, 1.5) as cathodes were prepared for electrolyte-cathode interfacial resistance measurement with SDC as electrolytes and $Y_{0.5}Ca_{0.5}BaCo_{4-x}Zn_xO_7$ ($x = 0.3$, 1.0, 1.5) as cathodes. SDC powders were first pressed at 300 MPa. The green compacts were then sintered at 1400 °C for 5 h. $Y_{0.5}Ca_{0.5}BaCo_{4-x}Zn_xO_7$ and SDC powders at a ratio of 1:1 were mechanically mixed with organic additives to form a slurry. The slurry was then applied to both sides of the sintered SDC electrolytes by screen-printing, and subsequently calcining at 1000 °C for 2 h to form porous electrodes. Silver current collector layer were prepared on both sides of the porous electrodes.

For single cell test, $Sm_{0.2}Ce_{0.8}O_{1.9}$ (SDC) and NiO powders were first mechanically blended (NiO:SDC = 60:40 wt.%) and pressed in a steel die. The green compacts were then fired at 1000 °C for 2 h. SDC electrolyte slurry was prepared onto the fired NiO/SDC substrates by a dip-coating method. The coated samples were then co-sintered at 1300 °C for 5 h to obtain anode/electrolyte bi-layer structure with dense SDC electrolyte film supported on porous NiO/SDC substrates. Single cells were finally obtained by screen-printing $Y_{0.5}Ca_{0.5}BaCo_3ZnO_7$-SDC slurry onto the electrolyte side of the NiO/SDC bi-layer and subsequently sintering at 1000 °C for 2 h [14]. The active area of the cathode in the single cells is 0.2376 cm^2.

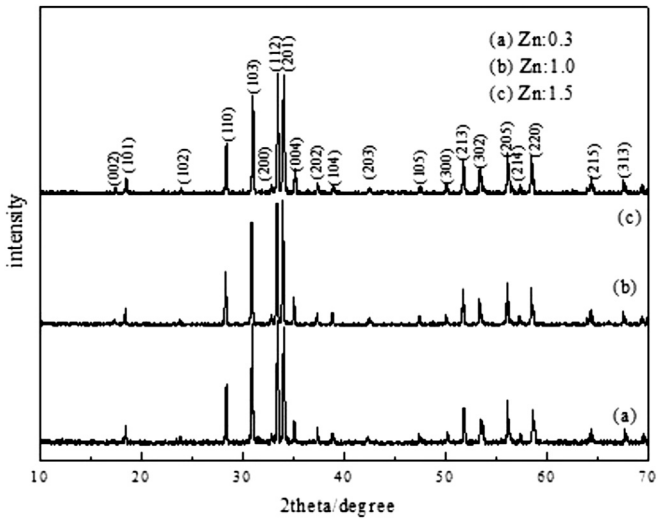

Fig. 1. XRD patterns of the $Y_{0.5}Ca_{0.5}BaCo_{4-x}Zn_xO_7$ powders calcined at 1000 °C for 2 h.

2.2. Characterization

Phase structure of the synthesized $Y_{0.5}Ca_{0.5}BaCo_{4-x}Zn_xO_7$ ($x = 0.3$, 1.0, 1.5) powders was determined by X-ray diffraction (XRD, Philips). Microstructure of the sintered samples was observed by scanning electron microscopy (SEM, JSM-6700F, JEOL). Electrical conductivity of the sintered $Y_{0.5}Ca_{0.5}BaCo_{4-x}Zn_xO_7$ ($x = 0$, 0.3, 1.0, 1.5) samples was measured using the four-probe dc method in temperature range of 400–800 °C with a digital multimeter (Keithley 2001). Thermal expansion coefficients (TEC) of the sintered samples were measured using a dilatometer (NETzsch DIL 402c). Area specific resistance (ASR) was measured with the symmetrical cells using two-probe method with electrochemical workstation (ZHANER im6ex). The measurements were conducted at 500–800 °C in air in the frequency range from 0.1 to 1 MHz with a bias voltage of 10 mV. Performance of the single cells was tested using a home-made fuel cell testing device with humidified hydrogen (−3% H_2O) as the fuel and ambient air as the oxidant. The current–voltage (I–V) and current-power (I–P) curves of the cells were also tested.

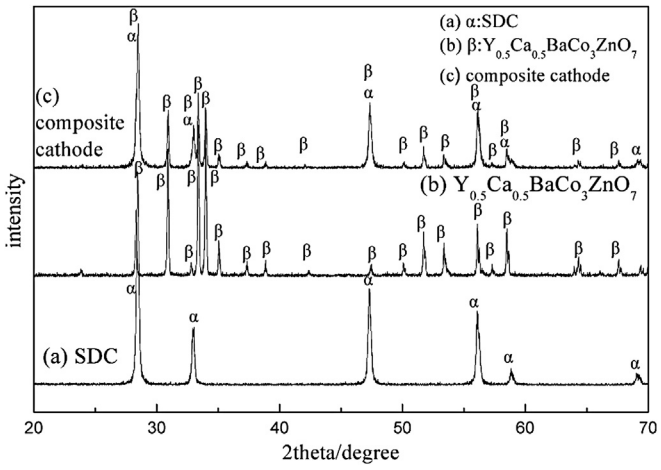

Fig. 2. XRD patterns of the $Y_{0.5}Ca_{0.5}BaCo_3ZnO_7$-SDC composite powders, the $Y_{0.5}Ca_{0.5}BaCo_3ZnO_7$ and SDC powders calcined at 1000 °C for 10 h, 1000 °C for 2 h and 800 °C for 2 h, respectively.

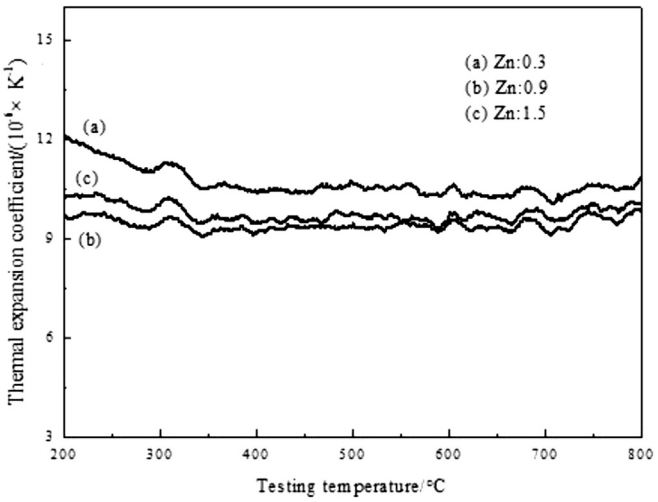

Fig. 3. Dependences of thermal expansion coefficients (TEC) of the sintered $Y_{0.5}Ca_{0.5}BaCo_{4-x}Zn_xO_7$ samples on test temperature in air.

3. Results and discussion

3.1. XRD analysis

Fig. 1 shows XRD patterns of the $Y_{0.5}Ca_{0.5}BaCo_{4-x}Zn_xO_7$ ($x = 0.3$, 1.0, 1.5) powders calcined at 1000 °C for 2 h. All the diffraction peaks are well indexed as $RBaCo_4O_7$ structures, which is in agreement with literature report, where the crystal lattice was identified as hexagonal phase with space group of $P6_3mc$ [5,15]. This indicates that moderate substitution of Co by Zn and Y by Ca in $YBaCo_4O_7$ materials does not change their phase structure.

To evaluate the chemical stability of the $Y_{0.5}Ca_{0.5}BaCo_{4-x}Zn_xO_7$–$Sm_{0.8}Ce_{0.2}O_{1.9}$ (SDC) composite cathode materials, $Y_{0.5}Ca_{0.5}BaCo_3ZnO_7$–SDC (50:50) powder mixtures were calcined at 1000 °C for 10 h for XRD analysis, Fig. 2 shows XRD patterns of the calcined $Y_{0.5}Ca_{0.5}BaCo_3ZnO_7$–SDC composite powder. For comparison, XRD patterns of pure $Y_{0.5}Ca_{0.5}BaCo_3ZnO_7$ and SDC were also shown in Fig. 2. Only peaks corresponding to $Y_{0.5}Ca_{0.5}BaCo_3ZnO_7$ (hexagonal structure) and SDC (cubic fluorite structure) are observed in the XRD patterns of $Y_{0.5}Ca_{0.5}BaCo_3ZnO_7$–SDC composite powders sintered at 1000 °C for 10 h. This suggests that there are no observable chemical reactions between $Y_{0.5}Ca_{0.5}BaCo_3ZnO_7$ and SDC after co-firing them at 1000 °C for 10 h, and it can be deduced that the composite cathode materials possess good chemical stability at 1000 °C.

3.2. Thermal expansion coefficients

Fig. 3 shows thermal expansion coefficients (TEC) of the $Y_{0.5}Ca_{0.5}BaCo_{4-x}Zn_xO_7$ ($x = 0.3$, 1.0, 1.5) samples in temperature range of 200–800 °C. Average TEC values of the $Y_{0.5}Ca_{0.5}BaCo_{4-x}Zn_xO_7$ specimens are 11.2×10^{-6} K^{-1}, 9.3×10^{-6} K^{-1} and 9.7×10^{-6} K^{-1} for the compositions of $x = 0.3$, 1.0 and 1.5, respectively. The low TEC values of the $Y_{0.5}Ca_{0.5}BaCo_{4-x}Zn_xO_7$ materials, especially $Y_{0.5}Ca_{0.5}BaCo_3ZnO_7$ composition, are comparable to those of some electrolyte materials such as doped ceria, YSZ, etc. The substitution of Zn for Co in the lattice significantly improves the structural stability, which may be caused by the absence of spin–state transition in the $Co^{2+/3+}$ ions accompanied by the loss of oxygen with temperature.

3.3. Electrical conductivity

Fig. 4 shows the dependence of electrical conductivity of $Y_{0.5}Ca_{0.5}BaCo_{4-x}Zn_xO_7$ ($x = 0$, 0.3, 1.0, 1.5) samples on temperature in 400–800 °C in air. Electrical conductivity of all samples has a positive temperature coefficient with a typical semiconducting behavior in whole temperature range (Fig. 4a). However, Fig. 4a shows that while the samples with $x = 0$ (no Zn doping) have electrical conductivity of 40.16 and 61.19 Scm^{-1} at 600 °C and 800 °C, respectively, the samples with $x = 0.3$, $x = 1.0$, $x = 1.5$ have electrical conductivity of 25.92, 12.23 and 3.73 Scm^{-1} at 600 °C, and 40.33, 20.87 and 7.05 Scm^{-1} at 800 °C, respectively. This indicates that Zn doping amount has an adverse influence on the electrical conductivity of $Y_{0.5}Ca_{0.5}$ $BaCo_{4-x}Zn_xO_7$ materials, which may be attributed to the decrease of the concentration of charge carrier caused by the substitution of Co by Zn. Activation energy for electrical conduction can be calculated from the slope of the Arrhenius plots (Fig.4b), where the ln (σT) is plotted versus 1000 T^{-1} according to the Arrhenius equation:

$$\sigma = \frac{A}{T}\exp\left(-\frac{E_a}{kT}\right)$$

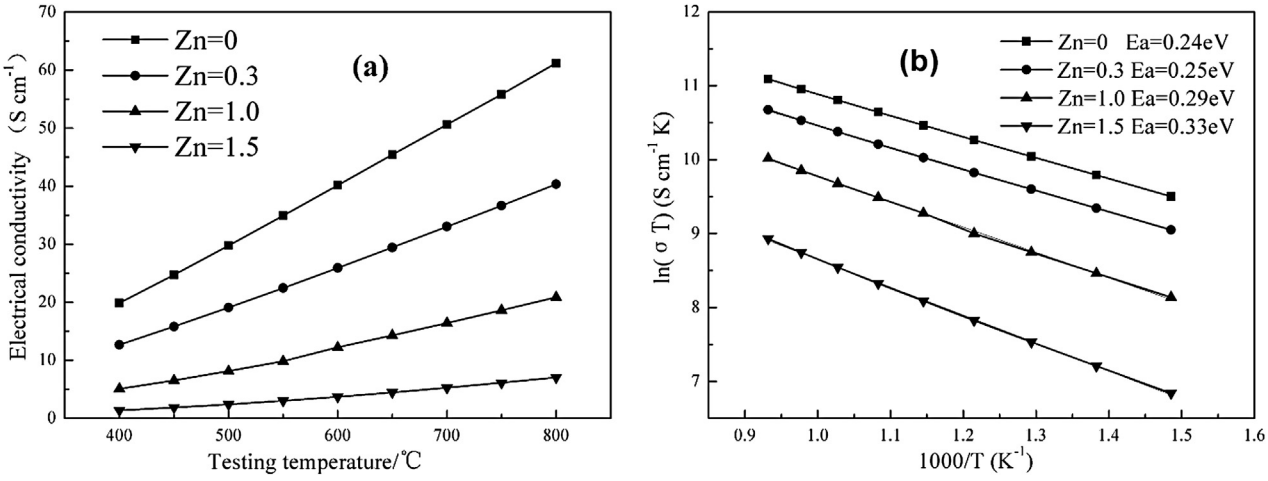

Fig. 4. Electrical conductivity (a) and Arrhenius plots of the conductivity (b) of the $Y_{0.5}Ca_{0.5}BaCo_{4-x}Zn_xO_7$ samples as a function of testing temperature.

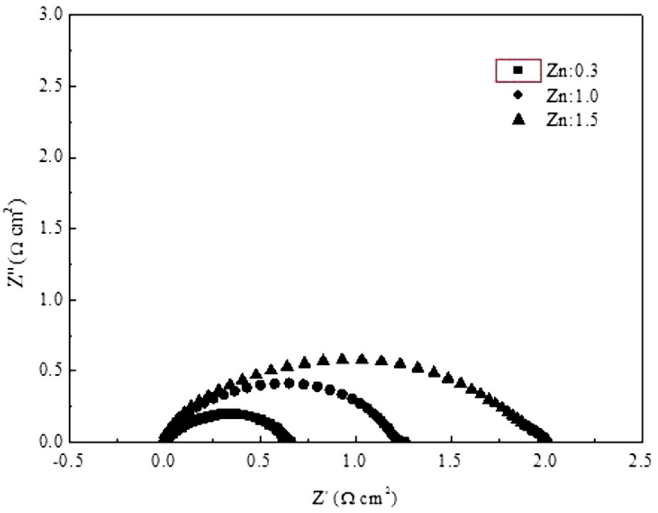

Fig. 5. Impedance spectra of $Y_{0.5}Ca_{0.5}BaCo_{4-x}Zn_xO_7$ (x = 0.3, 1.0, 1.5) materials measured under open-circuit condition at 750 °C in air.

where A is the pre-exponential factor containing a carrier concentration term, T is the absolute temperature, κ is the Boltzman factor and E_a is the activation energy.

It was calculated that activation energy of electrical conduction is in the range of 0.24–0.33 eV for the test samples, and the values increase with Zn doping amount. This may be caused by two factors. Firstly, in small polaron hopping conduction, small polarons migrate from one lattice site to an adjacent lattice site [16]. The activation energy mainly comes from the barriers encountered by the hopping holes. When Zn partially substitutes for Co in the lattice, the distance of hopping becomes larger and the lattice parameters increase with the Zn content, which may lead to the increase of barrier height [12]. Secondly, the activation energy of $YBaCo_4O_{7+\delta}$ materials increases with the decrease of δ value, which suggests that the oxygen contents have effects on activation energy in R114 system [17].

3.4. Electrochemical performances

The AC impedance spectroscopy of the symmetrical cells with $Y_{0.5}Ca_{0.5}BaCo_{4-x}Zn_xO_7$ materials was measured and the results

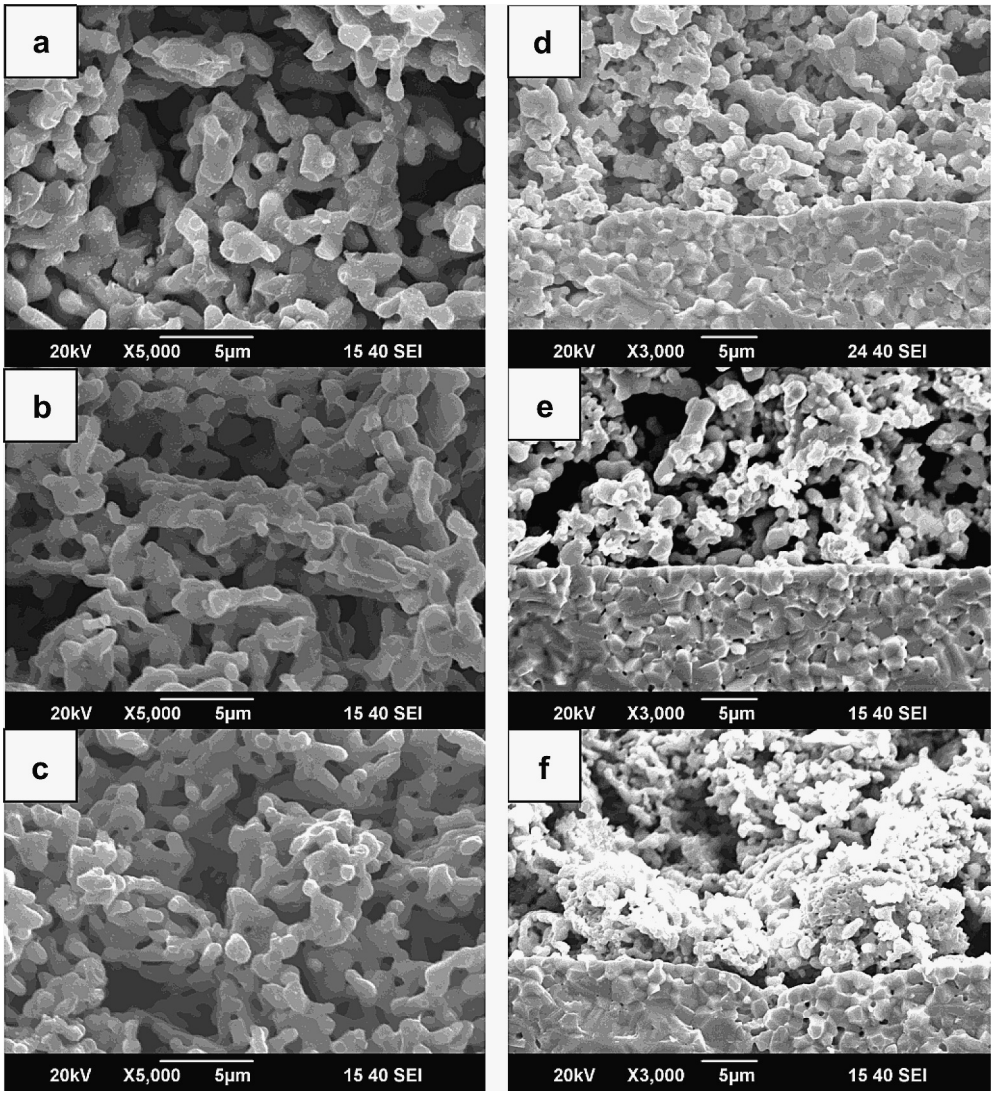

Fig. 6. Microstructure of the $Y_{0.5}Ca_{0.5}BaCo_{4-x}Zn_xO_7$ and $Y_{0.5}Ca_{0.5}BaCo_{4-x}Zn_xO_7$-SDC (50:50) samples sintered at 1000 °C for 2 h. (a), (b) and (c): $Y_{0.5}Ca_{0.5}BaCo_{4-x}Zn_xO_7$ with x = 0.3, 1.0, 1.5, respectively; (d), (e) and (f): $Y_{0.5}Ca_{0.5}BaCo_{4-x}Zn_xO_7$-SDC (50:50) with x = 0.3, 1.0, 1.5, respectively.

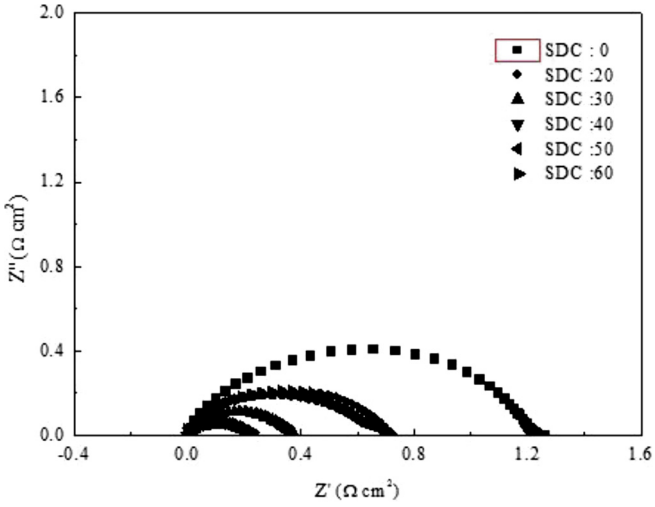

Fig. 7. Impedance spectra of $Y_{0.5}Ca_{0.5}BaCo_3ZnO_7$-SDC composite cathodes with different contents of SDC measured under open-circuit condition at 750 °C in air.

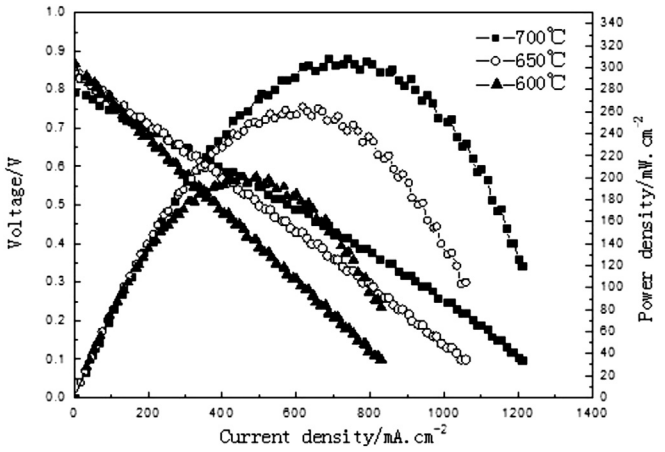

Fig. 9. I–V–P curves of a single cell consisting of a SDC electrolyte, a composite $Y_{0.5}Ca_{0.5}BaCo_3ZnO_7$-SDC (50:50) cathode and a Ni-SDC anode.

were shown in Fig. 5. The high frequency intercept of the impedance spectra shows the ohmic resistance (R_Ω) of the cell, which includes resistance of the electrolyte, the electrodes, the current collectors and the silver wires. The intercept at low frequency gives the total resistance of the cell. In general, the total cathode polarization resistance (R_p) equals to half of the value of high frequency intercept subtracted by the low frequency intercept. The low polarization resistance from the electrode–electrolyte interfaces, contributing to R_p values, is beneficial to the improvement of the catalytic activity [18].

The R_p value of the symmetrical cells with a configuration of cathode ||SDC|| cathode was measured in air cell. In this work, the cathode polarization resistance was represented by area specific resistance (ASR). Fig. 5 shows impedance spectra for $Y_{0.5}Ca_{0.5}BaCo_{4-x}Zn_xO_7$ materials with $x = 0.3$, 1.0 and 1.5, respectively. The results indicate that substitution Zn for Co increases the value of R_p. Fig. 6a–c shows SEM microstructure of the sintered $Y_{0.5}Ca_{0.5}BaCo_{4-x}Zn_xO_7$ materials with different zinc doping amount (x). It is seen that as zinc doping amount increases, porosity of the sintered samples decreases. This may be due to the promoted sintering at high concentrations of Zn in lattice. Comparing Figs. 5 and 6a–c, it can be seen that, as zinc doping amount increases, the sintered samples become denser, which may reduce the triple-phase boundaries (TPB) and increases the cathode polarization resistance (R_p). On the other hand, from Fig. 4, Zn doping decreases the electrical conductivity, which may also lead to the increase of electrode polarization resistance.

Fig. 7 shows variation of impedance spectra measured under open-circuit conditions at 750 °C in air for the $Y_{0.5}Ca_{0.5}BaCo_3ZnO_7$-SDC composite cathodes with different DCO contents. It was shown that the overall size of the impedance arcs decreases with the increase of SDC contents. The impedance arc of pure $Y_{0.5}Ca_{0.5}BaCo_3ZnO_7$ cathode is a larger arc. However, the addition of SDC into $Y_{0.5}Ca_{0.5}BaCo_3ZnO_7$ materials reduces the electrode polarization, which may be due to the extension of the triple-phase boundaries (TPB) for the catalytic activity of oxygen reduction reaction (ORR) [19]. Moreover, SDC in the cathode enhances the ability of oxygen ions transfer and enlarged the electrochemical reaction zones [20].

The impedance spectra of the symmetric cells with $Y_{0.5}Ca_{0.5}BaCo_{4-x}Zn_xO_7$ ($x = 0.3$, 1.0, 1.5) -SDC (50:50) composite cathodes are shown in Fig. 8. The $Y_{0.5}Ca_{0.5}BaCo_3ZnO_7$-SDC (50:50) sample demonstrates the best performance among all the samples, which

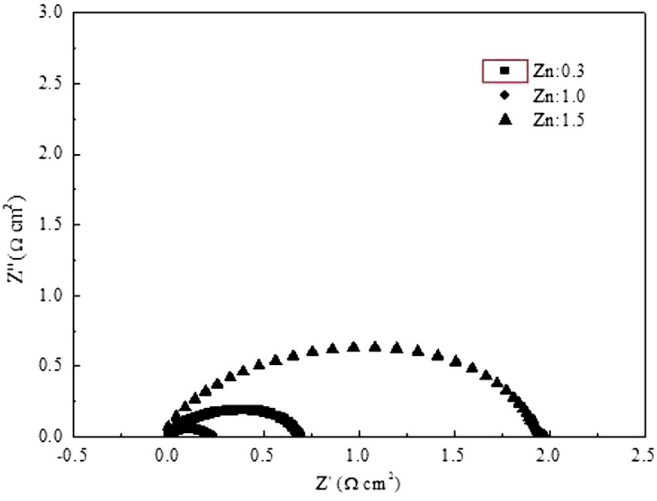

Fig. 8. Impedance spectra of $Y_{0.5}Ca_{0.5}BaCo_{4-x}Zn_xO_7$-SDC (50:50) composite cathodes with different Zn contents measured under open-circuit condition at 750 °C in air.

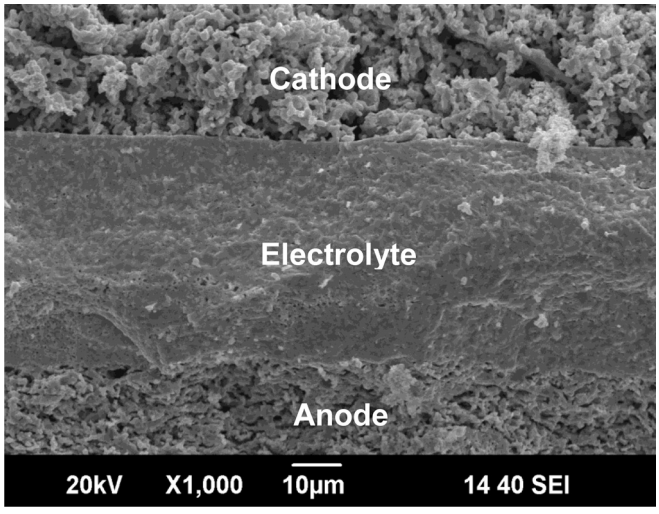

Fig. 10. Cross-section images of the single cell based on the $Y_{0.5}Ca_{0.5}BaCo_3ZnO_7$-SDC (50:50) composite cathode after test.

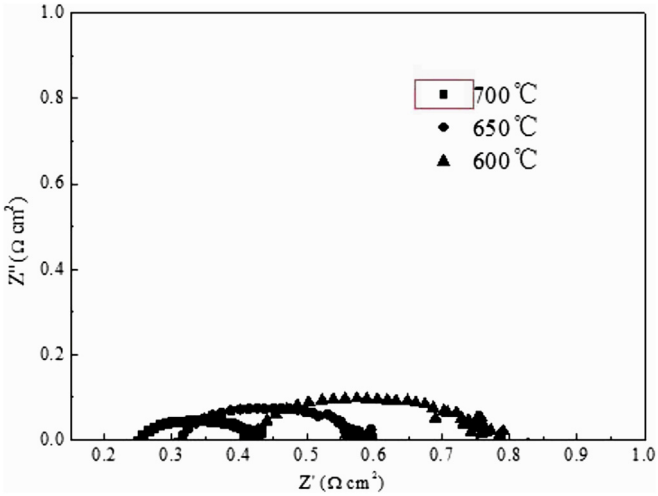

Fig. 11. AC impendence spectra of the single cell with a SDC electrolyte, a $Y_{0.5}Ca_{0.5}BaCo_3ZnO_7$-SDC (50:50) composite cathode and a Ni/SDC anode.

may be attributed to the porous microstructure as shown in Fig. 7d–f. The $Y_{0.5}Ca_{0.5}BaCo_3ZnO_7$-SDC (50:50) composite cathode shows homogeneous and more porous microstructure than other compositions, which is beneficial to the increase of triple-phase boundaries (TPB) and to the reduction of electrolyte polarization.

3.5. Cell performances

Single cells based on $Y_{0.5}Ca_{0.5}BaCo_3ZnO_7$-SDC (50:50) composite cathode were fabricated with SDC as electrolyte and NiO/SDC as anode. Thickness of the SDC electrolyte and the $Y_{0.5}Ca_{0.5}BaCo_3ZnO_7$-SDC composite cathode was about 40 μm and 30 μm, respectively. Fig. 9 shows power density and open circuit voltage (OCV) of the cell as a function of testing temperature. The cell shows a maximum power density of 320 mW cm^{-2} and a maximum OCV of 0.88 V, at 700 °C respectively. Fig. 10 shows cross-section microstructure of the single cell with the composite cathodes after test. Fig. 11 shows the total electrode polarization resistance including anode and cathode contribution. Total ASR value of the single cell tested is about 0.4 Ω cm^2.

4. Conclusions

$Y_{0.5}Ca_{0.5}BaCo_{4-x}Zn_xO_7$ powders with hexagonal structure were successfully synthesized by a combustion method. The doping amount of zinc has a great influence on the electrical conductivity, thermal expansion coefficients, as well as the electrochemical performances of the $Y_{0.5}Ca_{0.5}BaCo_{4-x}Zn_xO_7$ materials. The $Y_{0.5}Ca_{0.5}BaCo_{4-x}Zn_xO_7$ materials are chemically stable with SDC electrolytes even after co-firing at temperature around 1000 °C. $Y_{0.5}Ca_{0.5}BaCo_{4-x}Zn_xO_7$-SDC composite cathodes shows lower area specific resistances (ASR) than pure $Y_{0.5}Ca_{0.5}BaCo_{4-x}Zn_xO_7$ materials, and the $Y_{0.5}Ca_{0.5}BaCo_3ZnO_7$-SDC (50:50) samples have ASR of 0.05 Ω cm^2 at 800 °C and 0.11 Ω cm^2 at 750 °C, respectively. Single cells based on the $Y_{0.5}Ca_{0.5}BaCo_3ZnO_7$-SDC (50:50) composite cathodes with a 40 μm $Sm_{0.2}Ce_{0.8}O_{1.9}$ electrolyte film and NiO/SDC anodes show a maximum power density of 320 mW cm^{-2} at 700 °C. The present work has indicated that the $Y_{0.5}Ca_{0.5}BaCo_{4-x}Zn_xO_7$ materials and the $Y_{0.5}Ca_{0.5}BaCo_{4-x}Zn_xO_7$-SDC composite materials might be potential candidates for cathode materials of intermediate temperature solid oxide fuel cells.

Acknowledgments

This work is financially supported by the Natural Science Foundation of Anhui Province (contract No.070414186), the Program of Science and Technology of Anhui Province (contract No.2008AKKG0332), the Nippon Sheet Glass Foundation for Materials Science and Engineering (NSCF) (contract No. 070304B2) and the Open Project Program of Key Laboratory of Low Dimensional Materials & Application Technology (Xiangtan University), Ministry of Education of China under contract No. DWKF0802.

References

[1] M. Letilly, O. Joubert, A. Le Gal La Salle, J. Power Sources 212 (2012) 161.
[2] K. Świerczek, J. Power Sources 196 (2011) 7110.
[3] C.L. Yang, Q.M. Xu, J. Power Sources 212 (2012) 186.
[4] M. Valldor, M. Andersson, Solid State Sci. 4 (2002) 923.
[5] M. Valldor, Solid State Sci. 6 (2004) 251.
[6] H.S. Hao, J.H. Cui, C.Q. Chen, L.J. Pan, J. Hu, X. Hu, Solid State Ionics 177 (2006) 631.
[7] M. Valkeapää, M. Karppinen, T. Motohashi, R.S. Liu, J.M. Chen, H. Yamauchi, Chem. Lett. 36 (2007) 1368.
[8] E.V. Tsipis, D.D. Khalyavin, S.V. Shiryaev, K.S. Redkina, P. Núñez, Mater. Chem. Phys. 92 (2005) 33.
[9] J.H. Kim, A. Manthiram, Chem. Mater. 22 (2010) 822.
[10] V.B. Vert, J.M. Serra, J.L. Jordá, Electrochem. Commun. 12 (2010) 278.
[11] S. Kadota, M. Karppinen, T. Motohashi, H. Yamauchi, Chem. Mater. 20 (2008) 6378.
[12] M.F. Liu, L. Zhao, D.H. Dong, S.L. Wang, J.D. Wu, X.Q. Liu, G.Y. Meng, J. Power Sources 177 (2008) 451.
[13] H.S. Hao, X.T. Zhang, Q.L. He, C.Q. Chen, X. Hu, Solid State Commun. 141 (2007) 591.
[14] F. Tietz, V.A.C. Haanappel, A. Mai, J. Mertens, D. Stöver, J. Power Sources 156 (2006) 20.
[15] H.S. Hao, C.Q. Chen, L.J. Pan, J.X. Gao, X. Hu, Physica B 387 (2007) 98.
[16] R.S. Singh, T.H. Ansari, R.A. Singh, B.M. Wanklyn, Mater. Chem. Phys. 40 (1995) 173.
[17] M. Karppinen, H. Yamauchi, S. Otani, T. Fujita, T. Motohashi, Y.H. Huang, M. Valkeapaa, H. Fjellvag, Chem. Mater. 18 (2006) 490.
[18] M. Balaguer, V.B. Vert, L. Navarrete, J.M. Serra, J. Power Sources 223 (2013) 214.
[19] Y. Li, M.W. Xu, J.B. Goodenough, J. Power Sources 209 (2012) 40.
[20] Q.J. Zhou, W. Wang, T. Wei, X.L. Qi, Y. Li, Y.L. Zou, Y. Liu, Z.P. Li, Y. Wu, Ceram. Int. 38 (2012) 1529.